Al-Rafidain Journal of Engineering Sciences

Journal homepage https://rjes.iq/index.php/rjes

ISSN 3005-3153 (Online)

Structural Behaviour of Reinforced Concrete Flat Plate with Double Steel Plates as Shear-head

Mohammed Mohammed Rasheed[1], and Wadhah M. Tawfeeq[2]

[1] Department of Civil Engineering, Al Mustansiriyah University, Baghdad, Iraq
[2] Department of Civil Engineering, Sohar University، Sohar, Oman

ARTICLE INFO

Article history:

Received	28 June 2025
Revised	30 June 2025
Accepted	23 July 2025
Available online	27 July 2025

Keywords:
Flat plate
Punching shear
Double plate
Studs shear-head

ABSTRACT

This paper presents an experimental investigation on the behavior of punching shear of flat plate reinforced concrete slabs with double steel plates as shearhead. Five reinforced concrete square slabs of 70 mm thickness were confirmed as four edges simply supported by a 900 mm span length and tested under a static concentrated load at the center of the slab. The proposed shearhead consists of double rectangular steel plates (sandwiched, at top and bottom) connected by four studs, and installed at each column side in the column-slab connection area. The effect of steel plates length (90 mm and 180 mm) and thickness (2 mm and 4 mm) have been investigated through studying their effect on crack pattern, failure mode, load-deflection behavior, ultimate loads, elastic stiffness, and absorbing energy. Specimen SB2 (with steel plate of 180 mm length and 4 mm thickness) has the best enhancement in ultimate load, elastic stiffness, and absorbing energy by 29.5, 268, and 92 %, respectively, in comparison with the reference slab without shear reinforcement. Also, the experimental values of punching shear strength were compared with the proposed equation of design codes (ACI and EC2). In comparison with the experimental results, the prediction equations of codes show conservative values for slabs without shear reinforcement, and good agreement results for slabs with shear reinforcement.

1. Introduction

A flat plate is a reinforced concrete slab built without beams, girders, drop panels, or column capitals, and is supported without delay on columns [1]. This structural member has gained popularity in multi-story construction production because of several sensible and monetary benefits. Among these, the capacity to create thinner ground sections and acquire flat ceiling finishes sticks out as the number one benefit. The absence of drop panels and beams simplifies the formwork, leading to faster and more economical construction. In addition, this gadget provides architectural flexibility, as columns can be positioned more freely to fit the construction's layout, making it suitable for office buildings, resorts, hospitals, cars parking, and many structures. The decreased story height accomplished via the usage of flat plates contributes to a lower in the normal constructing height, which in flip reduces façade costs, elevator journey distances, and wind masses, consequently improving ordinary production efficiency and constructing performance.

Despite these advantages, flat plates are inherently at risk of a brittle and probably catastrophic failure mode known as punching shear. Punching shear occurs at the slab-column connection while the localized compressive strain across the column exceeds the slab's shear potential, resulting in a

Corresponding author E-mail address: mmrk72@uomustansiriyah.edu.iq
https://doi.org/10.61268/27b7vq81

truncated cone-formed failure surface. This phenomenon is particularly important in interior column connections, where multidirectional shear forces act without the useful consequences of side confinement. If not well accounted for, punching shear can critically compromise the load-sporting potential of the slab device underneath gravity hundreds and might even cause modern disintegration in extreme cases. Given those risks, big research has been committed to information and enhancing the punching shear overall performance of flat slabs.

Numerous studies were carried out to analyze the parameters influencing punching shear energy, each in unreinforced slabs and slabs bolstered with diverse shear reinforcement strategies [2-4]. These studies have recognized important variables, such as slab thickness, column size, reinforcement ratio, concrete energy, and the presence of shear reinforcement. Among the sensible solutions proposed to enhance punching shear resistance are external strengthening strategies regarding metal plates, collars, and bolts. These techniques are especially beneficial for retrofitting existing buildings where unique designs have expanded or deficiencies have been detected. Experimental studies provided by many studies [5-7] have validated the effectiveness of such metallic-based retrofitting systems in redistributing stresses across the column location and enhancing load resistance. These interventions not handiest increase potential but also can delay or mitigate crack formation and propagation.

Moreover, the use of superior substances, such as fiber-reinforced polymer (FRP) composites, has emerged as a possible opportunity to replace steel materials for strengthening programs. These substances are lightweight, corrosion-resistant, and easy to put in. For instance, El-Kashif et al. (2019) [8] used carbon fiber-reinforced polymer (CFRP) laminates to enhance punching resistance in slab-column joints. The incorporation of FRP materials allows for tailored strengthening designs and added advantage of inflicting minimal disruption during installation.

In parallel with experimental advancements, simplified analytical models have been developed to estimate the punching shear. In general, most of the international design codes contain empirical equations derived from laboratory testing, which estimate punching capacity primarily based on shear perimeter, slab depth, concrete strength, and shear reinforcement [9, 10]. Also, researchers have proposed modified equations which include the contribution of extra reinforcement or strengthening for slabs [11-14].

Despite full-scale progress, the capability of the usage of double metal plate shear heads in a sandwich configuration remains unexplored in the literature. Most research recognition on stud rails and other shear connector sorts, with limited interest given to plate-primarily based structures. Furthermore, current design hints no longer explicitly don't forget such configurations, relying alternatively on popular-cause safety elements or empirical adjustments. This gap underscores the need for additional research into how those structures perform beneath realistic loading situations.

To deal with this expertise gap, current studies have begun to explore revolutionary strengthening techniques. Ibrahim & Fawzy (2023) [15] studied GFRP-based retrofitting of flat slabs, showing promising consequences in terms of each energy and ductility. Majeed & Abbas (2019) [16] evaluated the influence of shearhead collars, while Abood et al. (2024) [17] and Yan & Xie (2024) [18] added information-driven prediction equations for the calculationg punching shear. Satjapan et al. (2022) [19] and Saadoon et al. (2022) [20] investigated the mixing of recycled aggregate concrete and metallic fibers as a sustainable approach, and Abdulhussein & Al-Sherrawi (2021) [21] analyzed metallic collar upgrades. These contributions together spotlight the huge variety of answers presently under exploration.

In this study, a modern strengthening system, the usage of double metallic plates tied together with studs in a sandwich configuration, could be proposed for the slab-column interface. By varying the plate dimensions and thicknesses, this approach pursuits to improve the punching shear resistance, manipulate crack improvement, and provide a realistic strengthening solution that complements current techniques. Through experimental and analytical evaluation, the proposed gadget can contribute extensively to the advancement of flat plate protection and overall performance

2. Experimental Programs

2.1 Specimen details

The experimental work of this study includes tested five specimens of reinforced concrete flat plates. The first slab specimen is defined as (SR) and considered as a reference (without shear head). Other slabs (four slabs) are considered with shear head, reinforced by double plates (at top and bottom) connected by four studs fixed at each column side in column-slab connection area, as shown in Figure 1.

Two of specimens are defined as SA1 and SA2, strengthened by shear head type A of 2 mm and 4 mm thickness, respectively. The last two specimens are defined as SB1 and SB2, strengthened by shear head type B of 2 mm and 4 mm thickness, respectively, as shown in Figure 1.

All slabs are geometrically similar, having dimensions of (1000 × 1000 × 70 mm) and loaded through a central column of dimensions of (150 ×150 × 200 mm). The slabs have the same flexural reinforcement. Welded wire fabric mesh (Ø6 @ 75 mm) is used as flexural reinforcement placed in the bottom of the slabs. The slabs are simply supported along all edges and have a clear span of 900 mm.

Four shear connectors were used for each sandwich (to connect top and bottom steel plates) with a distance between shear connectors of 30 mm in longitudinal direction and 50 mm in lateral direction for shear head type A, and 60 mm in longitudinal direction and 50 mm in lateral direction for shear head type B. Clear cover of 10 mm from top and bottom was provided for shear connectors.

2.2 Material properties

- Cement: Ordinary Portland cement type I was used, and it conforms to the Iraqi Specification No.5 -2019 [22].
- Fine aggregate: natural sand was used, and it conforms to the Iraqi Specification No.45 -1984 [23]. The sand has a maximum size of 5 mm (zone 2) and a specific gravity of 2.68
- Coarse aggregate: crushed river gravel was used, and it conforms to the Iraqi Specification No.45 -1984 [23]. Used gravel has a grading of (5 – 14) mm and a specific gravity of 2.56
- Superplasticizer (SP): It is free from chlorides and specifies the ASTM C 494 [24] type F.
- Steel reinforcement: welded wire meshes were used as tensile flexural reinforcement with a yield strength of 577 MPa. The mesh consists of 6 mm diameter deformed wire distributed at 75 mm c/c in each direction.
- Steel plates: with yield strengths of 243 MPa and 312 MPa for plates of 2 mm and 4 mm, respectively.
- Shear connectors: steel studs of 8.5 mm diameter with a yield strength of 353 MPa were used as shear connectors, welded to the top and bottom steel plates.

2.3 Concrete mixture

The concrete is provided by mixing 450 kg of cement, 680 kg of sand, 1100 kg of gravel, a 0.35 w/c ratio, and 2% superplasticizer (by weight of cement) for one cubic meter. The compressive strength of the concrete was determined at 28 days by using cylindrical specimens (150 × 300) mm according to ASTM C39 [25], with the average compressive strength of 50 MPa. Table 1 shows the test results of concrete.

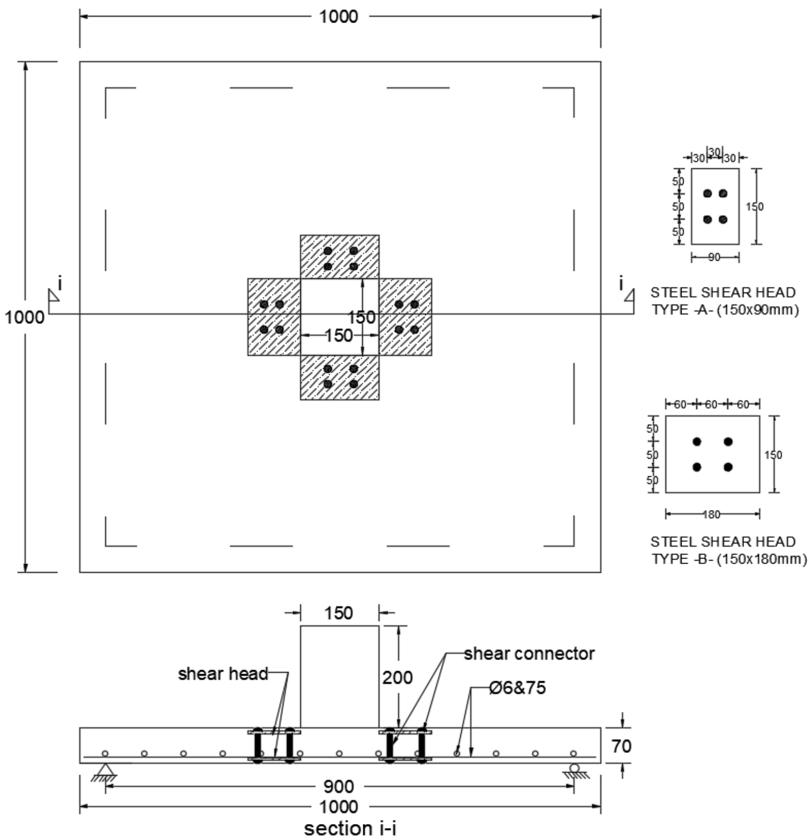

Figure 1. Details of the specimen

Table 1: Test mechanical results of concrete

Test type	Value*	Specification
Compressive strength (MPa)	50	ASTM C39-86 [25]
Splitting tensile strength (MPa)	4.44	ASTM C496-03 [26]
Modulus of Rupture (MPa)	4.66	ASTM C78-84 [27]
Static modulus of elasticity (MPa)	28946	ASTM C469-03 [28]

* Each value represents average of five tested specimens.

2.4 Test setup and loading procedure

A universal hydraulic machine of 3000 kN capacity was used to test the specimens. And special supporting frame was manufactured to install the slab specimen in this machine, as shown in Figure 2. The loading was provided as concentrated load with a 10 kN rate. The vertical deflection of the slab was recorded by using LVDT (Linear Variable Displacement Transducer) installed at the bottom face of slab at mid spans.

3. Results and discussion

3.1 Crack Pattern and Failure Mode

The conduct of a reinforced concrete flat plate or flat slab beneath loading may be divided into four distinct stages. The first stage, called the elastic behaviour level, starts with the application of the load, and continues till the first visible crack appears. The second stage, known as the cracking degree, extends from the formation of the preliminary crack to the onset of yielding; during this phase, flexural cracks increase throughout the slab. The third stage, or plastic behavior degree, starts while yielding begins and continues till the slab reaches its last flexural strength, which is about expected by the yield line principle. In this section, yielding of the tension reinforcement progresses outward from the loaded place in the direction of the slab edges. The fourth and final stage, referred to as the failure stage, is characterized by a plastic response wherein deflection will increase considerably without a corresponding growth in load [29]. Table 2 provides the consequences for each of the first cracking and final load capacities of the slabs.

Upon the utility of loading, the first crack commonly appears across the perimeter of the column region at the anxiety face of the slab, occurring at approximately 17–20% of the slab's closing load ability. Before the formation of this preliminary crack, all tested slabs exhibited comparable behavior, marked by surprisingly minor deformations.

The preliminary crack is commonly longitudinal and diagonal in form, forming below the loaded area at the tension side of the slab. As the weight continues to grow, additional longitudinal and diagonal cracks develop and enlarge outward from the initial cracking region closer to the slab edges. Simultaneously, the number of cracks intensifies around and close to the column location.

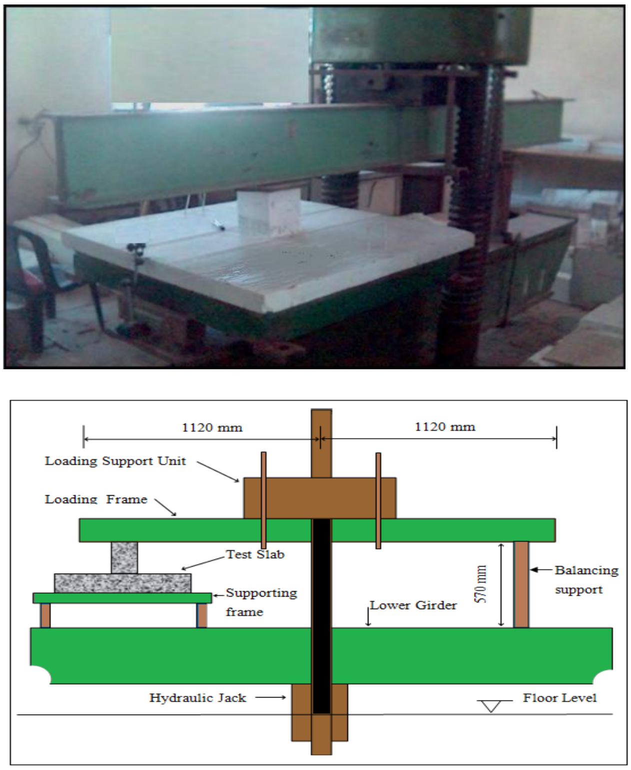

Figure 2. Test setup

With similar loading, the slabs subsequently experience full flexural and normal shear failure inside the aid region. This failure mode evolves right into a way shear mechanism under heavy loading. Notably, the slabs exhibited symptoms of imminent failure, which include a sudden boom in deflection measurements. Slabs incorporating a four mm thick metal plate failed predominantly in flexure, even as others exhibited punching shear failure. Figure 3 depicts the observed crack styles and failure modes.

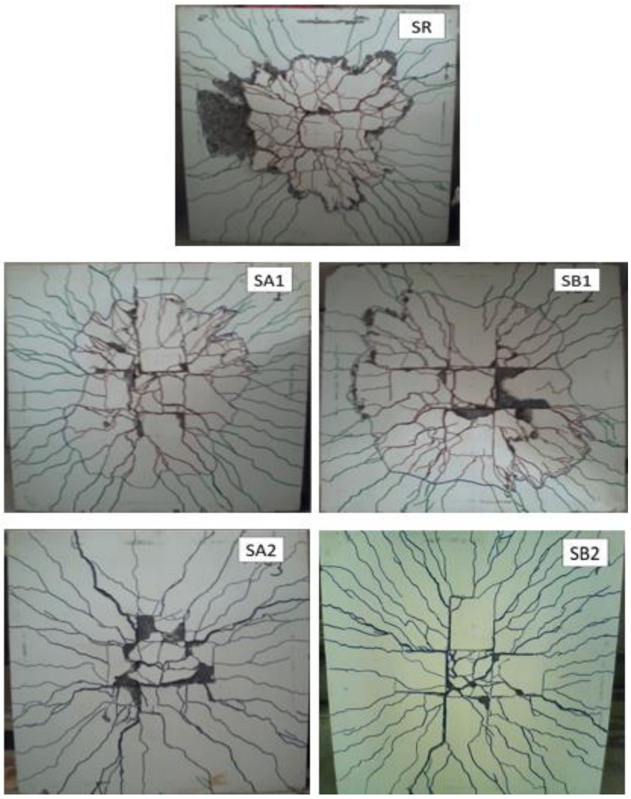

Figure 3. Crack patterns of tested slabs

3.2 Load-Deflection Behaviour

The load-deflection behaviour of the tested specimens is supplied in Figure 4, while Table 2 provides the corresponding vertical deflection values at specified load, the primary cracking load (Pcr), and the last load (Pu). As proven in Figure 4, all specimens exhibited similar common behavior as well as failure. The test results suggest that the best deflection at ultimate load turned into recorded for slabs utilizing Type B shear plates (SB1 and SB2). In contrast, the lowest deflection at last load was located within the slab with a Type A shear plate of 2 mm thickness (SA1). The findings can be summarized as follows:

Table 2: Results of tested specimens

Slab	P_{cr} (kN)	Δ_{cr} (mm)	P_u (kN)	Δ_u (mm)	P_{cr}/P_u %	Increasing in P_u%	Mode of failure
SR	40	2.30	173	23.12	19.51	-	Punching
SA1	38	1.25	201	24.02	18.91	16.18	Punching
SB1	42	2.05	205	27.17	20.49	18.50	Punching
SA2	38	0.87	218	26.45	17.43	26.01	Flexural
SB2	41	0.64	224	27.31	18.30	29.48	Flexural

Pcr: First crack load; Pu: Ultimate load; Δcr: Vertical deflection at Pcr; Δu: Vertical deflection at Pu.

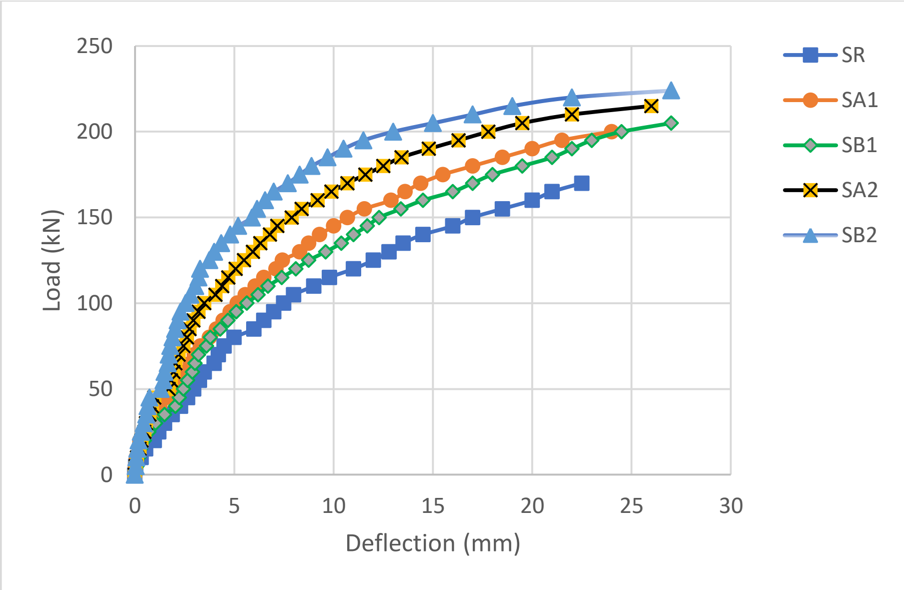

Figure 4. Load-Deflection Curves of Slab

1. In SA1 and SB1, both slabs are provided with the same sandwich plates of thickness 2 mm and the number of shear connectors but differ in the spacing between studs and plates' length. The deflection of SA1 and SB1 decreases by about 36.14% and 24.44%, respectively, in comparison with the deflection of the reference slab (SR) at ultimate load. SA1 at its ultimate load exhibits a decrease in deflection of about 2.04% less than the deflection of SB1.

2. In SA1 and SA2, both slabs are provided with the same spacing between shear connectors and dimension of sandwich plates, but with varied thicknesses of 2 and 4 mm, respectively. The deflection of SA1 and SA2 decreases by about 36.14% and 52.44%, respectively, in comparison with the deflection of the reference slab (SR) at ultimate load. The deflection of SA1 at its ultimate loads increases by about 34.83% more than SB2.

3. In SB1 and SB2, both slabs are provided with the same spacing between shear connectors and dimension of sandwich plates, but with varied thicknesses of 2 and 4 mm, respectively. The deflection of SB1 and SB2 decreases by about 24.44% and 65.78%, respectively, in comparison with the deflection of the reference slab (SR) at ultimate load. The deflection of SB1 at their ultimate loads increases by about 80.00% more than SB2.

4. In SA2 and SB2, both slabs are provided with the same sandwich plate thickness of 4 mm and number of shear connectors but differ in spacing between shear connectors and length of plates. The deflection of SA2 and SB2 decreases by about 52.44% and 65.78%, respectively, in comparison with the

Corresponding author E-mail address: mmrk72@uomustansiriyah.edu.iq
https://doi.org/10.61268/27b7vq81

deflection of the reference slab (SR) at ultimate load. The deflection of SA2 at their ultimate loads increases by about 36.84% more than SB2.

3.3 Ultimate Load

The foremost objective of this study is to evaluate the last load-carrying ability of slabs reinforced for punching shear and to examine their overall performance with that of a reference slab lacking such reinforcement. Table 2 offers the observed failure numbers for all tested specimens. Based on the experimental consequences, the subsequent key observations may be made:

1. In (SR), the punching shear failure occurs at the lower loads than the other slabs with steel plates. The test results of the slabs with shear head (SA1, SB1, SA2, and SB2) have obviously increased in strength over the reference slab (SR) by about 16.18, 18.50, 26.01 and 29.48 % respectively.
2. For SA1 and SB1, the increasing of ultimate load of SB1 is only about 1.99% greater than SA1.
3. For SA1 and SA2, the increasing of ultimate load of SA2 is only about 8.46% greater than SA1.
4. For SB1 and SB2, the increasing of ultimate load of SB2 is only about 9.27% greater than SB1.
5. For SA2 and SB2, the increasing of ultimate load of SB2 is only about 2.75% greater than SA2.

3.4 Elastic stiffness and absorbed energy

Elastic stiffness is defined as the slope of the linear part of the load deflection curve in the initial elastic range (until cracking load). Absorbed energy is defined as the whole area under the load deflection curve before failure (until the ultimate load)

The results of all slabs with shear head have elastic stiffness and absorbed energy greater than the reference slab (without shear head). Table 3 shows that slab SB4 has the maximum value of stiffness and energy compared with the others. In comparison with the reference slab, it has an increase in elastic stiffness and absorbed energy of about 268% and 92%, respectively

4. Proposed punching shear equations by codes

In this research, the value of punching shear strength force from experimental results will be compared with the proposed equations of ACI 318-19 and EC2 codes. The following descriptions explain the code equations for the case without shear reinforcement

4.1 ACI 318-19 code

In this code, the shear strength of a two-way slab can be determined by using Eq. (1)

$$V_c = \min of \begin{cases} 0.33\lambda\lambda_s\sqrt{f'_c} \\ 0.17[1+\frac{2}{\beta}]\lambda\lambda_s\sqrt{f'_c} \\ 0.083[2+\frac{\alpha_s d}{b_o}]\lambda\lambda_s\sqrt{f'_c} \end{cases} \quad (1)$$

Where:

λ: lightweight concrete factor. λ_s: Modification factor for size effect $\lambda_s = \sqrt{\frac{2}{1+0.004d}} \leq 1.0$

β: Ratio resulting from dividing the longest by the shortest column width. α_s: Constant value classified according to column position within the slab plate, for the corner (20), for the edge (30), and the interior (40).

b_o: Length taken as perimeter for critical section. For a slab without shear reinforcement, it will be formed at d/2 as a length coming out of the column interface.

4.2 EC2-2004 code

In this code, the shear strength of a two-way slab can be determined by using Eq. (2)

$$V_c = 0.18K\ (100\rho_{av}f_{ck})^{1/3} b_o d_{av} \quad (2)$$

Where:

$K = 1 + \sqrt{\frac{200}{d_{av}}}$, d_{av}: average effective depth,

b_o: A critical perimeter, positioned at (2d) from column face which equals =2(C1+C2+2πd), C1 and C2 represent columns dimensions.

Table 3: Elastic stiffness and absorbed energy

Slab	Ks (kN/mm)	Ks/ Ksr	En (kN.mm)	E/ Esr
SR	17.39	1.00	2524	1.00
SA1	30.4	1.75	3399	1.35
SB1	20.49	1.18	3813	1.51
SA2	43.68	2.51	4247	1.68
SB2	64.06	3.68	4850	1.92

Ks: Elastic stiffness index; Ksr: Elastic stiffness index for reference slab; En: Absorbed energy

Table 4: Experimental and code results of punching shear forces

Slab	P_{exp} (kN)	P_{ACI} (kN)	P_{ACI}/P_{exp}	P_{EC2} (kN)	P_{EC2}/P_{exp}
SR	173	86	0.50	77	0.45
SA1	201	135	0.67	166	0.83
SB1	205	190	0.93	237	1.16
SA2	218	135	0.62	166	0.76
SB2	224	190	0.85	237	1.06

Table 4 shows the experimental and theoretical values of punching shear forces for the tested slabs. As shown in Table 4, the values of shear strength predicted by codes are less than 50% of the experimental result for slabs without shear reinforcement. The values of the proposed code equation compared to experimental results increase with the increasing dimension of the shear head. For slabs SA1 and SA2, the predicted values of punching shear by the ACI code are the same, because the equation does not include the effect of plate steel. Also, EC2 does not include the effect of plate steel. The same point can be observed in both codes for SB1 and SB2. When the shear head length increased from 90 mm to 180 mm, the prediction value of ACI reached 93% from the experimental value of SB1. While the prediction value of EC2 is 116% of the experimental value of SB1.

5. Conclusion

Depending on the test results of this study, the following conclusions are obtained:

1- The preliminary crack bureaucracy around the sides of the column on the tension face of the slab at about 17.43% to 20.49% of the remaining load. As loading continues, additional cracks expand within the relevant area of the slab, becoming wider and more severe with growing load. At the closing load, failure occurs abruptly in the form of punching shear.

2- Slabs SA1, SB1, SA2, and SB2 reveal a will increase in closing load compared to the reference slab (SR) by using about 16.18%, 18.50%, 26.01%, and 29.48%, respectively.

3- The maximum last load is achieved when the shear plate has a thickness of 4 mm and the spacing between shear connectors is 60 mm, corresponding to a steel plate length of 180 mm.

4- Decreasing the vertical deflection of slabs (SA1, SB1, SA2, and SB2) by about (36.14, 24.44, 52.44, and 65.78) % respectively in comparison with reference slabs (SR) at their ultimate load.

5- The slab with steel plate of 2 mm thickness, and shear connector spacing between 30 mm and 60 mm (SA1 and SB1), the increasing in ultimate load is only 1.99%.

6- The slab with a steel plate of 90 mm length, and steel plate thickness changed from 2 mm to 4 mm (SA1 and SA2), the increase in ultimate load reaches 8.46%.

7- The slab with a steel plate of 4 mm thickness, and shear connector spacing between 30 mm and 60 mm (SA2 and SB2), the increase in ultimate load is only 2.75%

8- The slab with steel plate of 180 mm length, and steel plate thickness changed from 2 mm to 4 mm (SB1 and SB2), the increasing in ultimate load reaches to 9.27%.

9- The tested results of punching shear strength were compared with the prediction equations proposed by ACI 318 and EC2 codes. These prediction equations were conservative in specimens without shear reinforcement. And give good agreement with specimens with shear reinforcement. In general, these equations did not include the effect of thickness or specification of the steel plate shear head.

Author Contributions

All authors have equally contributed to this paper. All authors have read and agreed to the published version of the manuscript.

Conflicts of interest

The authors declare no conflict of interests.

References

[1] P. Bhatt, T.J. MacGinley, and B.S. Choo, Reinforced concrete – Design theory and examples. 3rd ed. Publisher: Taylor & Francis, London, UK, 2006.

[2] D.R. Oliveira, G.S. Melo, and P.E. Regan, "Punching strengths of flat plates with vertical or inclined stirrups," ACI Structural Journal, vol. 97, no.3, pp. 485–491, 2000. DOI: 10.14359/4643

[3] S. Lips, M.F. Ruiz, and A. Muttoni, "Experimental investigation on punching strength and deformation capacity of shear-reinforced slabs," ACI Structural Journal, vol. 109, no. 6, pp. 889–900, 2012. https://doi.org/10.14359/51684132

[4] S.M. Allam, "Effect of shear reinforcement on punching shear strength of reinforced concrete slabs," International Review of Civil Engineering, vol. 4, no.5, pp. 253–264, 2013.

[5] P.G. Fernández, A. Marí, and E. Oller, "Theoretical prediction of the punching shear strength of concrete flat slabs under in-plane tensile forces," Engineering Structures 229, 111632, 2020. https://doi.org/10.1016/j.engstruct.2020.111632

[6] H.A. Ali, and M.H. Al-Sherrawi, "Steel collar strengthening of a slab-column connection under eccentric load," Engineering, Technology and Applied Science Research, vol. 14, no.4, pp. 14677–14684, 2024. https://doi.org/10.48084/etasr.7391

[7] J.S. Al-Abasi, M.M. Rasheed, and M.A. Yaseen, "Experimental study of lightweight concrete flat plate with sandwich shear plates," Journal of Engineering and Development, vol. 16, no. 4, pp. 107–126, 2012. https://jeasd.uomustansiriyah.edu.iq/index.php/jeasd/article/view/1143

[8] K.F. El-Kashif, E.A. Ahmed, and H.M. Salem, "Experimental investigation of strengthening slab-column connections with CFRP fan," Ain Shams Engineering Journal, vol. 10, no.3, pp. 639–650, 2019. https://doi.org/10.1016/j.asej.2019.02.005

[9] American Concrete Institute (ACI), ACI-318, Building code requirements for structural concrete and , commentary, USA, 2019.

[10] European Committee for Standardization (CEN), Eurocode 2: design of concrete structures – part 1-1: General rules and rules for buildings. European Committee for Standardization. Brussels. 2001

[11] R.T.S. Mabrouk, A. Bakr, and H. Abdalla, "Effect of flexural and shear reinforcement on the punching behavior of reinforced concrete flat slabs," Alexandria Engineering Journal, vol. 56, no.4, pp. 591–599, 2017. https://doi.org/10.1016/j.aej.2017.05.019

[12] M.A. Golham, and A.H.A. Al-Ahmed, "Strengthening of GFRP reinforced concrete slabs with openings," Journal of Engineering, vol. 30, no.1, pp. 157–172, 2024. https://doi.org/10.31026/j.eng.2024.01.10

[13] M. Navarro, S. Ivorra, and F.B. Varona, "Parametric computational analysis for punching shear in RC slabs," Engineering Structures, vol. 65, pp. 254–263, 2018. https://doi.org/10.1016/j.engstruct.2018.03.035

[14] H.K. Ammash, S.S. Kadhim, and M.K. Dhahir, "Repairing half-loaded flat slabs against punching shear using steel stiffeners," Case Studies in Construction Materials 16, e01032, 2022. https://doi.org/10.1016/j.cscm.2022.e01032

[15] A.M. Ibrahim, and M.S. Fawzy, "Strengthening of RC flat slabs against punching shear with GFRP laminates adopting a hybrid technique," Engineering and Applied Science Research, vol. 50, no.5, pp. 490–498, 2023. https://ph01.tci-thaijo.org/index.php/easr/article/view/253016

[16] M.M. Majeed, and A.N. Abbas, "Punching shear strength characteristics of flat plate panels reinforced with shear-head collars: Experimental investigation," Civil Engineering Journal, vol. 5, no.3, pp. 528–539, 2019. https://doi.org/10.28991/cej-2019-03091265

[17] E.A. Abood, M.H. Abdallah, M. Alsaadi, H. Imran, L.F.A. Bernardo, D. De Domenico, and S.N. Henedy, "Machine learning-based prediction models for punching shear strength of fiber-reinforced polymer reinforced concrete slabs using a gradient-boosted regression tree," Materials, vol. 17, no.16, 3964, 2024. https://doi.org/10.3390/ma17163964

[18] H.J. Yan, and N. Xie, "Optimized machine learning algorithms for predicting the punching shear resistance of flat slabs with transverse reinforcement," International Journal of Concrete Structures and Materials, vol. 18, no.1, 76, 2024. https://doi.org/10.1186/s40069-024-00721-9

[19] L. Satjapan, I. Thanongsak, S. Monthian, G. Reyes, and K. Boksun, "Punching Shear Capacity of Recycled Aggregate Concrete Slabs," Buildings vol. 12, no.10, 1584, 2022. https://doi.org/10.3390/buildings12101584

[20] A.M. Saadoon, M.A. Mashrei, K.A. Al Oumari, "Punching shear strength of recycled aggregate-steel fibrous concrete slabs with and without strengthening," Advances in Structural Engineering, vol. 25, no.10, pp. 2175–2190, 2022. https://doi.org/10.1177/13694332221090288

[21] A.A. Abdulhussein, and M.H. Al-Sherrawi, “Experimental and numerical analysis of the punching shear resistance strengthening of concrete flat plates by steel collars,” Engineering, Technology and Applied Science Research, vol. 11, no.6, pp. 7853–7860, 2021. https://doi.org/10.48084/etasr.4497

[22] Iraqi specifications (No. 5-2019), Portland cement. Iraqi Central Organization for Standardization and Quality Control, 2019.

[23] Iraqi specifications (No. 45-1984), Aggregates from natural sources for concrete and building construction. Iraqi Central Organization for Standardization and Quality Control, 1984.

[24] ASTM C494M, Standard specification for chemical admixtures for concrete. ASTM International, 2017.

[25] ASTM C39, Test method for compressive strength of cylindrical concrete specimens. ASTM International, 1986.

[26] ASTM C469a, Test method for static modulus of elasticity and Poisson's ratio of concrete in compression. ASTM International, 2003.

[27] ASTM C78, Test method for flexural strength of concrete. ASTM International, 1984.

[28] ASTM C496, Standard test method for splitting tensile strength of cylindrical concrete specimens. ASTM International, 2003.

[29] S. Lulu, S. Yuanxie, and L. Shixue, “Reliability Analysis of RC Slab-Column Joints under Punching Shear Load Using a Machine Learning-Based Surrogate Model,” Building, vol. 12, no.10, 1750, 2022. https://doi.org/10.3390/buildings12101750